Off-Center Atomic Displacements in Zinc-Blende Semiconductor

Su-Huai Wei, S. B. Zhang, and Alex Zunger
National Renewable Energy Laboratory, Golden, Colorado 80401

(Received 30 October 1992)

We have studied theoretically the conditions for the occurrence of spontaneous off-center atomic displacements in pure zinc-blende semiconductors. A pseudo Jahn-Teller coupling of a chemically active valence d band with an s-like conduction band is predicted to lead to such a metastability. All-electron density functional calculations confirm that this is the case in CuCl. The unusual experimental manifestations of this metastability are outlined.

PACS numbers: 61.72.−y, 66.30.Dn, 77.22.Ej, 78.30.−j

When partially occupied orbitals are involved, tetrahedral semiconductors tend to exhibit rather complex bond-breaking structural rearrangements. This includes reconstructions at surfaces and off-center atomic displacements in deep defects such as the GaAs:Si$^-$ ("DX") center [1], the Si vacancy [2], and transition metal impurities in semiconductors [3]. Yet, the structural chemistry of the pure bulk tetrahedral semiconductor is exceedingly uneventful: Their fourfold tetrahedral coordination resists moderate pressures, isovalent alloying, and even amorphization. In this work we investigate the conditions for off-center structural instabilities (or metastability) *in pure crystalline tetrahedral semiconductors.* We predict that such instabilities will occur in the IB-VII semiconductors (e.g., CuCl and CuBr) as a result of a pseudo Jahn-Teller s-d coupling between conduction and valence bands. Its unusual experimental implications are outlined.

The general theoretical framework for testing the stability of a given structure with respect to atomic displacement Q is to examine the expansion of the ground state electronic energy $E_0(Q)$ with Q [4]:

$$E_0(Q)=E_0(0)+F_{0,0}Q+\tfrac{1}{2}(K_s+K_v)Q^2+\cdots . \quad (1)$$

Here, the linear vibronic force $F_{0,0}=\langle\Psi_0|\partial H/\partial Q|\Psi_0\rangle$ associated with the orbitally degenerate electronic states will lead to the usual first-order Jahn-Teller distortions when $F_{0,0}<0$. These are seen, e.g., in the charged Si vacancy [2], many transition-metal impurities in semiconductors [3], and *divalent* Cu d^9 compounds [4]. This term vanishes, however, in the closed-shell A_1-symmetric ground state akin to all pure octet semiconductors. The second-order term in Eq. (1) consists of two parts. The first, $K_s>0$, is the static (s) elastic force constant representing hindrance to the motion of nuclei in the frozen ground state electron distribution. The second term, K_v, represents charge relaxation due to the displacement-induced vibronic (v) coupling between the ground states Ψ_0 and excited states Ψ_i,

$$K_v=-2\sum_{i\neq 0}\frac{|F_{0,i}|^2}{E_i-E_0}, \quad (2)$$

where $F_{0,i}=\langle\Psi_0|\partial H/\partial Q|\Psi_i\rangle$ is the nondiagonal vibronic matrix element. Since this coupling lowers the ground state energy, $K_v<0$ [4]. The overall sign of the second-order term depends on both K_s and K_v. Soft modes ($K_s+K_v\approx 0$) or second-order (pseudo) Jahn-Teller distortions ($K_s+K_v<0$) are hence possible when the vibronic coupling competes favorably with classic restoring forces.

Equations (1) and (2) suggest that one should search for structural instabilities in intrinsically "soft" semiconductors (K_s small), having low-lying excited states that couple strongly to the ground state through an appropriate displacement ($|K_v|$ large). Consider, therefore, the states near the valence band (VB) maximum and conduction band (CB) minimum in zinc-blende semiconductors. While the states near the CB minimum are generally made up of atomic s orbitals, the states near the top of the VB are generally anion p-like in IV-IV and III-V semiconductors, anion p- and cation d-like in IIB-VI semiconductors [5], and mostly cation d-like in IB-VII systems [6]. Since the vibronic matrix elements $F_{0,i}$ of Eq. (2) are larger for s-d than for s-p coupling [4], we will initially focus on IIB-VI and IB-VII semiconductors. To search for a small energy denominator we examine the $E(d^{10})-E(d^9s^1)$ interconfigurational total energy difference measured in atomic spectroscopy [7]. This difference has a minimum at the top of column IB of the periodic table, i.e., 2.7 and 4.8 eV in Cu and Ag, respectively, while the IIB elements Zn, Cd, and Hg have larger barriers of 9.7, 10.0, and 5.3 eV, respectively. Photoemission and optical studies in IB-VII [8] and IIB-VI [5] semiconductors further confirm that the CB(s) − VB(d) difference reaches a minimum in Cu halides. This unique periodic table location of Cu at the end of the transition series, combined with the existence of chemically active d bands [6] and soft bonds [9] in zinc-blende Cu halides, suggests searching for a displacive instability in these systems. Indeed, the coordination chemistry of Cu d^{10} salts often exhibits small energy barriers separating different local bonding arrangements. This is manifested by ionic conductivity in Cu and Ag halides [10], the distorted tetrahedral units found in $Cu_4X_4Y_4$ cubanes [11] (interpreted qualitatively in terms of pseudo Jahn-Teller coupling [12,13]), and by the observation of photoinduced dielectric anomaly [14] and two sets of zone-center phonons in CuCl [15]. Despite many first-principles band structure calculations on IIB-VI [5] and IB-VII [6] semiconductors, no calculations on symmetry-lowering atomic displacements have been reported.

The symmetry requirement for a nonzero $F_{0,i}$ in Eq. (2) is that Q be contained in the direct product $\Gamma_{\Psi_0}\otimes\Gamma_{\Psi_i}$. This requirement and our foregoing discussion suggest searching for a symmetry-allowed displacement pattern that enhances the overlap between the *d* orbitals on a given metal atom and *s* orbital on a neighboring metal atom. Examples include cation motion along the threefold [111] axis of the tetrahedron. Figure 1 shows the change in total energy as a single atom is displaced along the [111] direction in a supercell model for Cu halides, the IIB-VI compound CdTe, a Zn substitution in CdTe, and the III-V compound GaAs. These were obtained using the local density approximation as implemented by the linear augmented plane wave method [16] using the Ceperly-Alder exchange correlation as parametrized by Perdew and Zunger [17]. We use a **k**-point sampling which is equivalent to ten special **k** points in the zinc-blende zone and four, eight, and sixteen atom supercells. Comparing the last two we find that the convergence error with respect to supercell size is ~0.02 eV per moving atom. For CuCl we find that atomic relaxation of all atoms at each Q lowers the energy by <0.05 eV per cell; however, the general feature of the energy curve is unchanged.

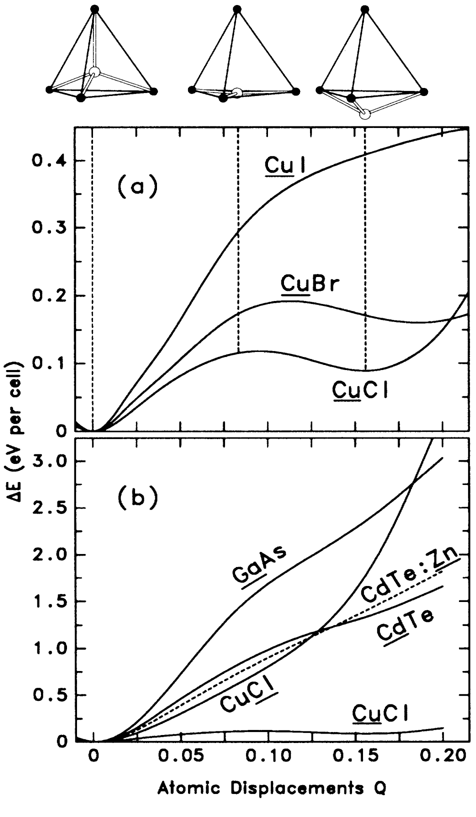

FIG. 1. The change in total energy as a function of [111] atomic displacement Q (in units of $\sqrt{3}a$) in a number of zinc-blende semiconductors. The underlined element is the one displaced.

Figure 1 shows that (i) a [111] Cu displacement in CuCl leads to an overall minimum at the tetrahedral site ($Q=0$). It is separated by a low-energy barrier E_b at $Q_b=0.095$ (in units of $\sqrt{3a}$) from a second, off-center minimum at $Q_0=0.156$ at an energy Δ_0 above the global minimum. This off-center minimum at Q_0 corresponds to a Cu position *below* the trigonal face (at $Q=0.083$). This geometry is analogous to that predicted for the GaAs:Si$^-$ *DX* center [1] and the *EL*2:As$_{\mathrm{Ga}}$ center [18]. While the distortion in *EL*2 can be thought of as resulting from a pseudo Jahn-Teller coupling of occupied *s* with empty *p* states, the relaxation in the *DX* center is an extrinsic effect, caused by *additional* electron doping from the conduction band into a defect level in the gap. (ii) As one moves in the series CuCl → CuBr → CuI, both Q_0 and the energies Δ_0 and E_b increase. (iii) CdTe and GaAs do not exhibit an off-center minimum upon cation displacement. This is also the case for Zn displacement in CdTe:Zn and for *anion* displacements (e.g., Cl in CuCl).

Figure 2 shows the $\bar{\Gamma}$-point energy levels as a function of Q for CuCl and GaAs. Figure 3 depicts the corresponding charge density contours for CuCl. In undistort-

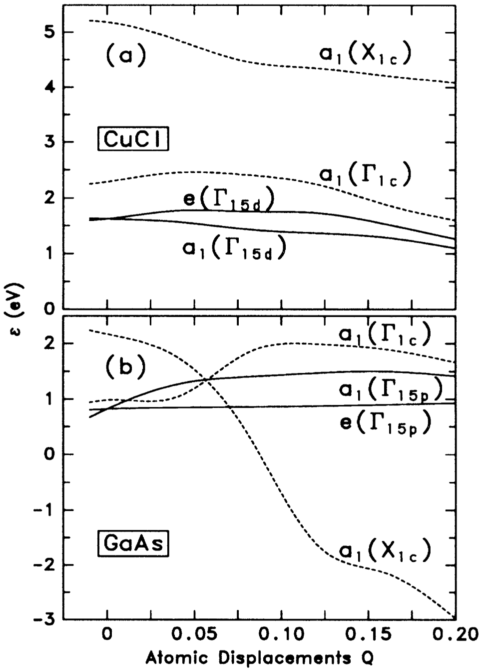

FIG. 2. Change in the $\bar{\Gamma}$-point energy levels as a function of atomic displacement Q for (a) CuCl and (b) GaAs. The label on each curve indicates the symmetry as well as (in parentheses) the dominant zinc-blende character. The states are connected according to these characters.

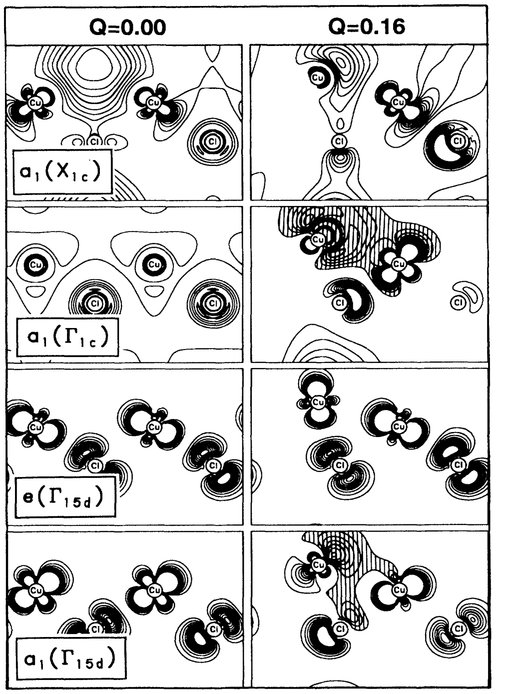

FIG. 3. Charge density contour plots for the CuCl states of Fig. 2(a) at $Q=0$ and 0.16.

ed CuCl the VB maximum is the threefold degenerate $t_{2d}(\Gamma_{15d})$ state; the empty CB minimum is a $a_1(\Gamma_{1c})$ s-like state. As the Cu atom is displaced towards the trigonal face, the a_1 states $a_1(\Gamma_{1c})$ and $a_1(X_{1c})$ drop in energy, while the $t_{2d}(\Gamma_{15d})$ state splits into $e+a_1$ with e below a_1 [19]. The charge densities shown in Fig. 3 and their decomposition into orbital components reveal that as Cu is displaced the occupied $e(\Gamma_{15d})$ valence state, owing to its symmetry, remains chemically inactive, but the occupied $a_1(\Gamma_{15d})$ valence state mixes with the empty $a_1(\Gamma_{1c})$ conduction band forming a Cu-Cu bond (shaded area in Fig. 3). This builds up s character on the *moving* (M) Cu atom ($\mathrm{Cu_M}$) and d character on the static (S), next-neighbor Cu atoms ($\mathrm{Cu_S}$). Initially, when Q is small, the $\mathrm{Cu_M}(s)$-$\mathrm{Cu_S}(d)$ interaction is weak because of the large $\mathrm{Cu_M}$-$\mathrm{Cu_S}$ separation. In this case the total energy increases with Q due to the large elastic restoring forces K_s. When Q increases further, the $\mathrm{Cu_M}$-$\mathrm{Cu_S}$ distance is reduced. This increases the overlap between the $\mathrm{Cu_M}(s)$ and $\mathrm{Cu_S}(d)$ states [$a_1(\Gamma_{1c})$ and $a_1(\Gamma_{15d})$]. The lowering in total energy due to this $\mathrm{Cu_M}(s)$-$\mathrm{Cu_S}(d)$ coupling eventually overwhelms the (anharmonicity-reduced) classic elastic energy, at which point the deformed system is stabilized. The causal relation between the s-d coupling and off-center displacement was further tested in a calculation in which *all* Cu atoms were displaced simultaneously. Here, the $\mathrm{Cu_M}$-$\mathrm{Cu_S}$ distance remains fixed, so the s-d interaction does not change significantly with Q. No off-center minimum was found. The strong s-d coupling between $a_1(\Gamma_{1c})$ and $a_1(\Gamma_{15d})$ is also manifested by the fact that the band gap variation with Q is relatively small in CuCl [Fig. 2(a)]. Note that the deeper energy anion p state $t_2(\Gamma_{15p})$ has an indirect role in this coupling: It displaces the Cu $t_2(\Gamma_{15d})$ state *upwards* through the p-d repulsion [5], thus reducing the $a_1(\Gamma_{1c})-a_1(\Gamma_{15d})$ energy difference which enhances s-d coupling. These observations confirm that the off-center minimum results from a displacement-enhanced coupling between the occupied d states and the empty s states, i.e., a second-order Jahn-Teller effect.

A similar mechanism explains the trends in the CuCl → CuBr → CuI series as well as the lack of off-center instability upon *anion* displacement. As one moves along the CuX series, the lattice constant increases and the d character at the top of the VB decreases, so the $\mathrm{Cu_M}(s)$-$\mathrm{Cu_S}(d)$ coupling decreases. As a result, the position Q_0 of the off-center minimum shifts to a larger value, and Δ_0 and E_b increase. Similarly, when the anion is displaced, the Cu-Cu distance is unchanged, so the s-d coupling remains weak and no off-center minimum is observed.

The IIB-VI and III-V systems present a case where the s-d coupling is too weak to stabilize an off-center minimum. In these compounds, the cation d orbitals are deeper in energy and significantly more localized, so the VB maximum is dominated by anion p states. As the cation is displaced along the [111] direction the $a_1(X_{1c})$ state drops in energy [Fig. 2(b)]. However, the coupling between this state and the cation $a_1(\Gamma_{15d})$ state is insignificant because of the large energy denominator of Eq. (2). The coupling with the anion $a_1(\Gamma_{15p})$ state is also very weak [4]. These effects permit the $a_1(X_{1c})$ defect state to continue dropping in energy and eventually become occupied. The total energy *increases* monotonically as a function of Q due to the dominance of the elastic energy. No off-center minimum is found.

Our foregoing discussion suggests that enhancing the s-d coupling will further stabilize the off-center distortion. We simulate this by a localized Cu $d \rightarrow \mathrm{CB}(s)$ photoexcitation process [20]. A supercell is created in which a d electron from the moving Cu atom is excited to the CB (the remaining $N-1$ atoms are in their d^{10} ground state configuration). This initial density is then iterated to self-consistency, keeping a hole in $\mathrm{Cu_M}$. Figure 4 shows that the lowest energy position is now at the off-center site.

Our prediction of an off-center displacement in CuCl would lead to a number of unique physical properties: (i) [111] cation displacements will lower the site symmetry from T_d to C_{3v}, thus creating a bond-oriented dipole moment. At high temperature the four equivalent [111] minima will be equally populated as particles tunnel dynamically between these minima. As the temperature is lowered, dipole correlations could lock in a net polarization, which should be observed as a dielectric anomaly. (ii) Our calculation confirms qualitatively the hypothesis

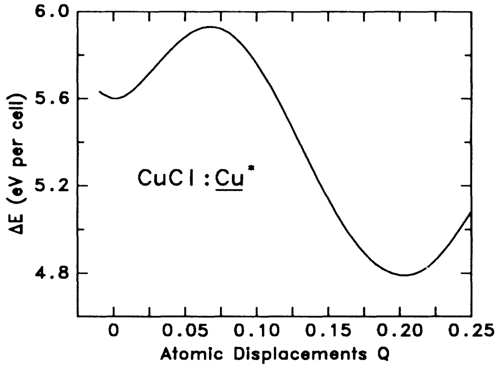

FIG. 4. The change in total energy as a function of [111] atomic displacement Q (in units of $\sqrt{3}a$) of an excited Cu atom (Cu*) in CuCl. The energy zero corresponds to the ground state of CuCl.

of Ref. [15] that the two sets of LO phonons observed in CuCl could result from large cationic displacements. Further quantitative comparison is difficult because, to determine the anomalous phonon mode, it requires total energy and force calculation of larger cell sizes than those treated here. However, our calculated trend in the CuCl→CuBr→CuI series is consistent with the observation [15] that while CuCl has a clear Γ-point phonon anomaly, this disappears in CuI. (iii) The physical properties of CuCl samples are predicted to depend on their thermal history which determines the distribution of particles in the two types of energy minima. Our model suggests that to enhance the fraction of atoms exhibiting phonon anomalies in CuCl, one should *heat* the sample (overcoming E_b), then quench it (trapping at Q_0), rather than going directly to low temperatures [15]. Furthermore, since the barrier $E_b - \Delta_0$ is smaller than the barrier E_b, we expect that the return of the trapped Cu atoms to the T_d site will be activated in an intermediate temperature range. (iv) Figure 4 suggests that when the electron-hole recombination rate is slow, photoexcitation can enhance the population of atoms in the off-center minima through tunneling of the Cu atom in the excited state and subsequent decaying to the metastable configuration. This is consistent with the observed photoinduced dielectric anomalies [14] and suggests that persistent photocapacitance quenching should be observable in CuCl.

We thank K. M. Rabe for useful discussions. This work was supported in part by the U.S. Department of Energy, Grant No. DE-AC02-83-CH10093. One of us (A.Z.) would like to thank the U.S.-Israel Binational Science Foundation (BSF) Grant No. 89-00324 for partial support and L. Benguigui, R. Kalish, and R. Weil for their discussions and hospitality.

---

[1] D. J. Chadi and K. J. Chang, Phys. Rev. Lett. **61**, 873 (1988); D. J. Chadi and S. B. Zhang, J. Electron. Mater. **20**, 55 (1991). See also *Proceedings of the International Symposium on DX Centers, Mauterndorf, Austria* [Semicond. Sci. Technol. **6** (1991)].

[2] G. A. Baraff, E. O. Kane, and M. Schluter, Phys. Rev. B **21**, 3563 (1980).

[3] A. Zunger, in *Solid State Physics*, edited by H. Ehrenreich and D. Turnbull (Academic, New York, 1986), Vol. 39, p. 275.

[4] I. B. Bersuker, *The Jahn-Teller Effect* (Plenum, New York, 1984).

[5] S.-H. Wei and A. Zunger, Phys. Rev. B **37**, 8958 (1988), and references therein.

[6] A. Zunger and M. L. Cohen, Phys. Rev. B **20**, 1189 (1979), and references therein.

[7] C. E. Moore, in *Atomic Energy Levels*, NBS, National Standards Reference Data Series—35 (U.S. GPO, Washington, DC, 1970).

[8] A. Goldmann, Phys. Status Solidi (b) **81**, 9 (1977).

[9] R. M. Martin, Phys. Rev. B **1**, 4005 (1970).

[10] J. B. Boyce, T. M. Hayes, and J. C. Mikkelsen, Phys. Rev. B **23**, 2876 (1981).

[11] G. L. Soloveichik *et al.*, Inorg. Chem. **31**, 3306 (1992).

[12] J. K. Burdett and O. Eisenstein, Inorg. Chem. **31**, 1758 (1992).

[13] S. Lee, P. Colombet, and G. Ouvrard, Inorg. Chem. **27**, 1291 (1988).

[14] I. Lefkowitz *et al.*, Ferroelectrics **73**, 487 (1987).

[15] Z. Vardeny and O. Brafman, Phys. Rev. B **19**, 3276 (1979); G. Livescu and O. Brafman, *ibid.* **34**, 4255 (1986).

[16] S.-H. Wei and H. Krakauer, Phys. Rev. Lett. **55**, 1200 (1985), and references therein.

[17] D. M. Ceperly and B. J. Alder, Phys. Rev. Lett. **45**, 566 (1980); J. P. Perdew and A. Zunger, Phys. Rev. B **23**, 5048 (1981).

[18] D. J. Chadi and K. J. Chang, Phys. Rev. Lett. **60**, 2187 (1988).

[19] The order of split $e(\Gamma_{15d})$ and $a_1(\Gamma_{15d})$ levels in this quantitative calculation is the opposite of what was anticipated in Ref. [12].

[20] A. Zunger, Phys. Rev. Lett. **50**, 1215 (1983).